^{2}H-NMR Imaging of Stress in Strained Elastomers†

M. Klinkenberg, P. Blümler, and B. Blümich*

Institut für Makromolekulare Chemie, Rheinisch-Westfälische Technische Hochschule Aachen, Worringerweg 1, 52074 Aachen, Germany

Received June 4, 1996; Revised Manuscript Received October 29, 1996⊗

ABSTRACT: ^{2}H NMR was used to image stress in strained elastomer bands made from natural rubber. Deuterated poly(butadiene) oligomers were incorporated into the rubber network by swelling. They act as spy molecules for probing the local chain orientation. Under uniaxially applied stress, the chain motion becomes anisotropic and the deuterium resonance is split into a doublet. The quadrupole splitting was spatially detected in two ways. Spectroscopic 2D imaging was used to acquire a spectrum for each spatial position. From each spectrum the line splitting was extracted and recalibrated to stress. A similar result could be achieved by the analysis of double-quantum (DQ) filtered images. Here, the image contrast is determined by the amplitude of the DQ signal, the spin density, and relaxation effects. The influence of the last two can be removed to yield images in which the contrast is determined only by the strength of the DQ coherence which passes the DQ filter. The quadrupole splitting can be extracted from a set of such images, and subsequent recalibration also leads to stress images. The first method can easily be implemented and is experimentally robust, but it suffers from low sensitivity to small strains while strong signals from isotropic regions restrict the dynamic range of the measurement. The second method is very sensitive to small strains, but only qualitative information is obtained unless a whole set of differently filtered DQ images is evaluated.

Introduction

NMR imaging has become a valuable instrument in medical diagnostics since its introduction in the early eighties. In recent years, NMR imaging is gaining increased acceptance in materials research.[1,2] An important advantage of NMR imaging, compared with other methods for the analysis of materials, is the possibility of investigating whole objects in a nondestructive fashion. A further remarkable feature is the large number of NMR parameters that can be used for the generation of image contrast.[3]

Elastomers are materials particularly suitable for NMR imaging because their chain mobility is high, so that standard NMR imaging techniques can be used. Due to the industrial significance of elastomers, investigations of the spatial strain distribution in such materials is very important. Stretched rubber bands, for example, have been investigated with T_2 parameter NMR imaging.[4] Inhomogeneities in the sample could clearly be distinguished, and stress images were obtained by recalibration of the image contrast with experimental T_2, stress, and strain values. The basic problem in the determination of stress in this way is the fact that the tensorial property stress is mapped by a scalar property, the transverse relaxation time T_2, so that, essentially, information is obtained about the trace of the stress tensor only.

This problem can be overcome by ^{2}H (deuteron) NMR imaging. The NMR parameter dominating all other spin interactions is the quadrupolar interaction of ^{2}H which is also a tensorial property. In uniaxially stretched rubber bands, the motional averaging of the quadrupole coupling is incomplete, which results in a splitting of the isotropic signal.[5] With this method, poly(siloxane) networks[6−11] as well as poly(butadiene) and poly(isoprene) networks[12−22] have been investigated spectroscopically. Due to the low natural abundance of deuterium, either the network chains have to be deuterated, which opens up the possibility of selective deuteration and hence the investigation of special chemical groups of interest,[7,12,13] or deuterated solvents[5] or oligomers with a chemical structure similar to that of the network chains have to be incorporated into the network. Then, under an applied stress the quadrupole splitting is also observed. It has been shown that the behavior of the oligomer chains under applied stress is almost the same as that of the network chains themselves, which makes the use of such spy molecules extremely suitable to probe the network chain order.[9,14,23] If the spectroscopic information is combined with NMR imaging, the averaging of the NMR properties across the bulk will be restricted to the dimensions of a voxel which allows a more detailed characterization of the sample. Imaging of quadrupolar nuclei has already been reported for solids[24,25] and liquids.[26] Double-quantum (DQ) coherences were used in these studies either during an evolution period for increased spatial resolution with subsequent spectroscopic detection[24,25] or in a preparation sequence in order to select specific chemical structures which show double-quantum transitions.[26]

In this work, stress is monitored spatially in strained natural rubber bands, with deuterated poly(butadiene) oligomers incorporated into the polymer matrix. Stress is mapped by recalibration of the quadrupole splitting (QS) by means of a master curve. The spatial variation of the QS is determined by spectroscopic imaging and by analysis of DQ filtered signals. The investigations were done with different sample geometries. Cuts, inserted into the rubber bands, deliberately induced a stress distribution. Finally, the parameter images were compared to images of stress distributions that were simulated by finite element matrix (FEM) calculation.

Theory

In ^{2}H-NMR spectroscopy, deuterated, relaxed elastomers exhibit a single, homogeneously broadened line, because the quadrupolar interactions are averaged by fast, essentially isotropic molecular motion of the network chains. Under applied stress, the molecular motion becomes anisotropic on the time scale of the NMR experiment, and the averaging of quadrupolar

† Dedicated to Prof. F. Asinger on the occasion of his 90th birthday.

⊗ Abstract published in *Advance ACS Abstracts,* February 1, 1997.

S0024-9297(96)00817-0 CCC: $14.00

Table 1. Ogden Parameters Derived from Mechanical Stress−Strain Measurements of the Investigated NR Bands

i	μ_i	α_i
1	−0.2122	2.872
2	1.774×10^{-4}	7.753
3	0.9378	−5.181

interaction is incomplete. As a result a splitting $\Delta\nu$ of the resonance is observed, which is given by[13,27]

$$\Delta\nu = {}^3/_2\delta P_2(\cos\Psi)\langle P_2(\cos\theta)\rangle\langle P_2(\cos\Phi)\rangle \qquad (1)$$

where θ is the angle between the end-to-end vector of a statistical segment and the stretching direction, Ψ is the angle between the stretching direction and the applied magnetic field, Φ is the angle between the C−D bond and the end-to-end vector of a statistical segment, and $\langle ... \rangle$ denotes an ensemble average of time-averaged orientations of quadrupole coupling tensors. Thus, eq 1 is valid in the fast motion limit. δ is the quadrupole coupling constant and P_2 is the second Legendre polynomial, $P_2(\cos\theta) = {}^1/_2(3\cos^2\theta - 1)$. Averages of $P_2(\cos\theta)$ are taken into account for distributions of θ in space and time. $\langle P_2(\cos\theta)\rangle$ is the second moment of the orientation distribution function of chain segments and is referred to as the order parameter S.

Experimental Section

We have investigated elastic bands, made from natural rubber (NR), which were swollen to an oligomer content of 5 vol % with 1,4-deuterated poly(butadiene) oligomers of an average molecular weight of $M_w = 550$. The deuterated poly(butadiene) oligomers were synthesized by anionic polymerization of 1,1,4,4-tetradeuterated butadiene in cyclohexane at 38 °C with *sec*-butyllithium as initiator[12] in standard high-vacuum equipment. The determination of the average molecular weight was performed by analysis of the ^{1}H-NMR spectrum.[15] Due to the chain length and the small signal of the undeuterated monomer units, the signals of the end groups could clearly be distinguished and, hence, the molecular weight could be calculated. An additional M_w determination using GPC could not be carried out due to rapid curing of the oligomers on the column. The microstructure of the oligomer molecules was examined by quantitative evaluation of the IR spectrum.[28] This yielded a composition of 7% 1,2-monomer addition, 38% trans-1,4, and 55% cis-1,4 monomer addition, which confirmed earlier investigations.[12] The mechanical characterization of the NR band was performed by stress−strain measurements and evaluation of the data with the phenomenological description by Ogden:[29]

$$\sigma = \sum_{i=1}^{3} \frac{2\mu_i}{\alpha_i}(\lambda^{\alpha_i - 1} - \lambda^{-(\alpha_i/2)-1}) \qquad (2)$$

A fit of this function to the stress−strain data gave the parameters shown in Table 1.

For the NMR investigations the bands were stretched in a home-built broad-band probe, that allows draw ratios up to about $\lambda \equiv l/l_0 = 4$, where l_0 and l are the initial and final sample lengths. The samples had a thickness of about 1 mm in the unstretched state and were examined in the *x*,*y*-plane of the laboratory coordinate frame. Because $\mathbf{B}_0$ is along the *z*-direction, the angle Ψ between the stretching direction and the applied magnetic field was 90°. This leads to $P_2(\cos\Psi) = -{}^1/_2$, and with $\langle P_2(\cos\Phi)\rangle = -0.154$ (determined by simulation of a poly(butadiene) chain with 50% cis- and trans-1,4 units respectively[13]) eq 1 can be simplified, giving

$$\Delta\nu = {}^3/_4\delta 0.154S \qquad (3)$$

The quadrupole coupling constant for the oligomers used was measured to be $\delta = 161$ kHz. It was determined by the analysis of the Pake pattern while the sample was cooled below its glass transition temperature. Thus, with the knowledge of δ, the order parameter can directly be determined from the quadrupole splitting via eq 3. However, this has not been carried out since the order parameter has no practical meaning for the data evaluation below.

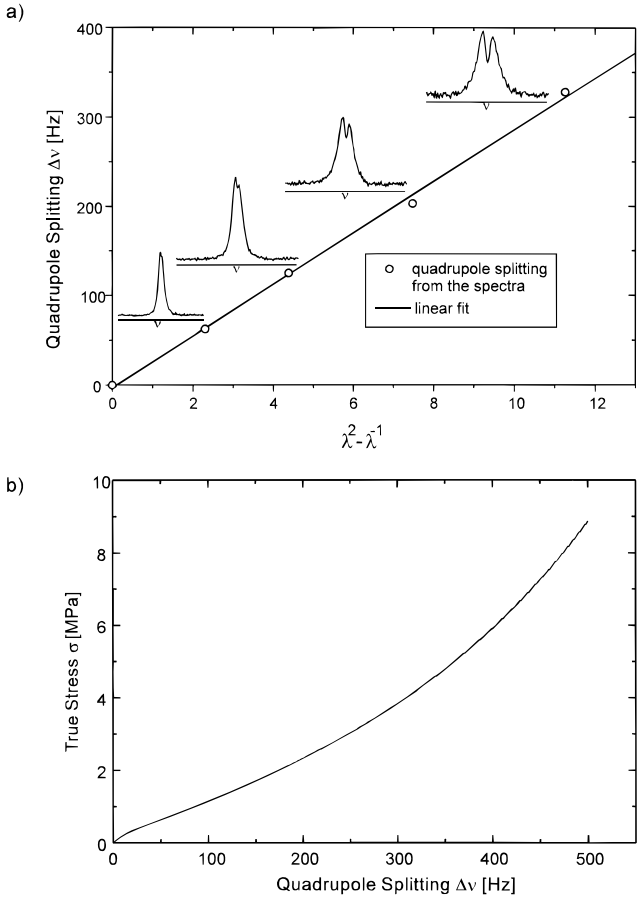

Figure 1. (a) Quadrupole splitting for different draw ratios λ plotted versus $\lambda^2 - \lambda^{-1}$. The measured spectra are depicted next to the extracted values. The line is a linear fit to the data. (b) Master curve used for recalibration of the quadrupole splitting to stress (using the values from Table 1).

All measurements were carried out on a Bruker CXP-200 NMR spectrometer at a ^{2}H resonance frequency of 30.8 MHz. The original Aspect 2000 computer had been replaced by a Macspect upgrade from Tecmag. The micro-imaging unit consisted of a home-built gradient coil system driven by two Techron amplifiers which were controlled by a home-built 8-bit digital-to-analog converter. The achieved spatial resolution in all images was 0.5 mm in both directions, with a field of view of 16 × 16 mm. The maximum achievable gradient strength was approximately 500 mT/m. Further experimental details are given elsewhere.[27]

Results and Discussion

Determination of the Master Curve. In order to determine the relation between quadrupole splitting and deformation, a homogeneously stretched elastic band was investigated. The draw ratio λ was varied, and from the acquired ^{2}H-NMR spectra the quadrupole splitting was extracted and plotted against $\lambda^2 - \lambda^{-1}$ (Figure 1a). This investigation at moderate strains yields a straight line, which confirms earlier investigations.[14,18] The second result of this investigation is the verification that poly(butadiene) oligomers are suitable spy molecules to probe a network made from natural rubber, though their chemical structure is not entirely

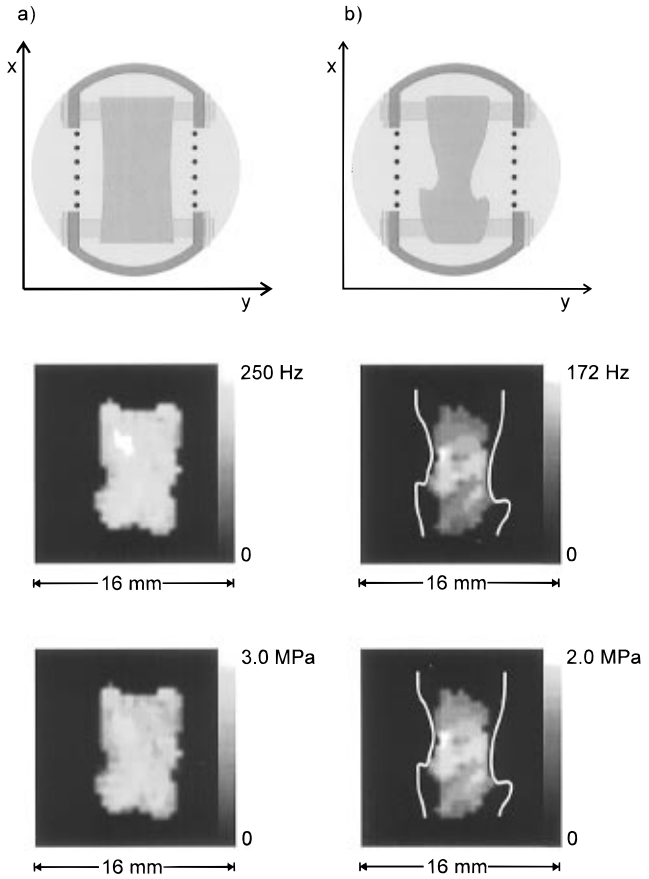

Figure 2. Top: sample arrangement in the probe of a homogeneously (a) stretched band at $\lambda = 2.7$ and a band with a cut on each side (b) at $\lambda = 1.5$. The dots mark the wire cross-sections of the flat rf coil. The $x-y$ plane is perpendicular to the applied magnetic field $\mathbf{B}_0$. Middle: spectroscopic 2D images of the samples. The contrast is determined by the quadrupole splitting. Bottom: stress parameter images obtained by recalibration of the corresponding spectroscopic 2D images. The contour obtained by integration over the spectra indicates the sample shape.

the same. With the parameters obtained by the stress–strain measurement and the subsequent evaluation according to Ogden, a master curve was derived which enables the recalibration of the QS data to stress data (Figure 1b). The swelling ratio was relatively small (<5%) and constant for all investigated samples. Therefore, a correction of the data of the swollen rubber with respect to the dry rubber was not necessary.

Spectroscopic Imaging. Two sample geometries were investigated (Figure 2). The top figures show a band homogeneously stretched to $\lambda = 2.7$ in the x-direction (a) and a band with a cut at each side (b) also stretched along the x-direction to $\lambda = 1.5$. The latter arrangement deliberately induces an inhomogeneous strain distribution for the purpose of demonstration.

Both elastic bands were investigated by spectroscopic 2D imaging.[27] A spectrum was acquired for each pixel, and the line splitting was extracted and used for contrast in Figure 2 (middle). These images were recalibrated to stress with the master curve of Figure 1b. The stress was then used as the contrast parameter (gray scale) in the images of Figure 2 (bottom). Although the stress distribution in the homogeneously stretched band should be narrow across the band, it is obvious that there are areas of high stress as well as areas of reduced stress. This can be accounted for by the existence of inhomogeneities inside the rubber.

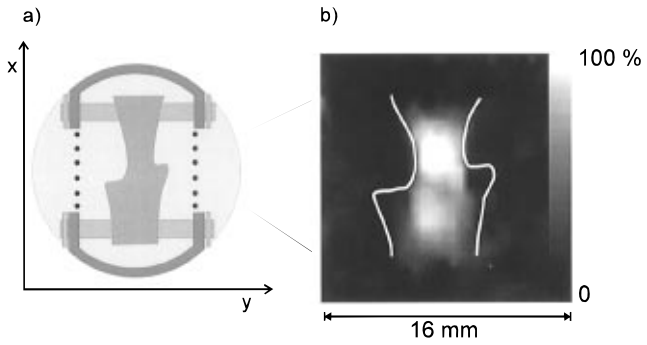

Figure 3. (a) Sample arrangement and (b) DQ weighted ^{2}H NMR image of a strained band with a cut on each side at $\lambda = 1.5$. The chosen setting of the DQ filter allows a qualitative evaluation of the image in terms of local stress. The outline obtained from a spin-echo image indicates the sample shape.

Inhomogeneous filler concentrations and cross-link densities, for example, are known to influence chain dynamics under stress.[4] The bottom figure of Figure 2b shows an image of the inhomogeneously stretched band. The narrow part in the middle exhibits the highest stress, whereas the stress decreases in the wider areas. This behavior is consistent with the geometry of the sample.

Some areas of low stress in the sample of Figure 2b seem to be "missing". This is due to the different sensitivity of the method to large and small stresses. The QS has to be larger than the width of the signal at half-height, and therefore, only a stress of $\sigma \geq 1.2$ MPa can be measured. Because there is no detectable QS, the "missing" areas stay blank.

Double-Quantum Filtered Imaging. For double-quantum (DQ) filtered imaging the magnetization was prepared by a DQ filter[30] ($90_x-\tau-180_y-\tau-90_x$) before the actual imaging sequence was applied. The signal strength is given by

$$S(\tau,\Delta\nu) \propto N_0 \sin(2\pi\tau\Delta\nu(\sigma)) \exp\left(\frac{-2\tau}{T_2(\sigma)}\right) \qquad (4)$$

where N_0 is the spin density and T_2 is the transverse relaxation time. Longitudinal relaxation effects are neglected in eq 4 because of their vanishing influence on the signal intensity. The value of τ determines the filter setting and thus the sensitivity of the filter to the different degrees of stress. Although the resulting images are only weighted by the DQ signal strength, with a proper choice of τ the signals for lower strain values decrease nonlinearly but monotonously.[27] Therefore, images for such a filter can be interpreted in a qualitative way. A DQ weighted image of a band with a cut on each side is depicted in Figure 3b for $\lambda = 1.5$ and a filter setting of $\tau = 600\ \mu$s. The contour outlining the sample shape in Figure 3b was taken from a spin-echo (SE) image. The areas with the highest strain in the narrow region of the band provide a strong signal in the DQ filtered image, while the signals from the unstrained lobes on both sides are attenuated. The intensity is not homogeneous over the sample, because the contrast is determined by the spin density, T_2, and the double-quantum coherence amplitude (cf. eq 4). However, the general intensity distribution is consistent with the geometry of the sample.

The effect of a DQ filter setting for which the signal intensity does not decrease monotonously with decreasing stress is demonstrated in Figure 4 where a band with a single cut was examined at $\lambda = 1.3$. The filter

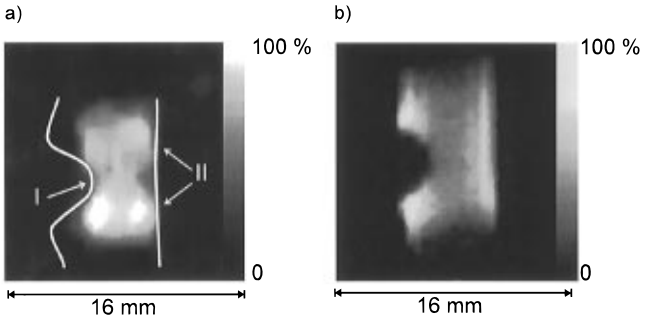

Figure 4. (a) DQ weighted ^{2}H NMR image of a strained band with a single cut at $\lambda = 1.3$. The DQ filter setting does not allow a qualitative evaluation of the image. Therefore, the area (I) in which the highest stress is expected does not show a high signal intensity, whereas the regions (II) with moderate stress exhibit the highest signal intensity. The outline obtained from a spin-echo image is shown to indicate the sample shape. (b) Spin-echo image of the same sample.

setting chosen in the DQ weighted image of Figure 4a results in regions with local draw ratios in the range $1.7 \leq \lambda \leq 2.7$ exhibiting almost the same signal intensity.[27] Again, the sample outline was taken from the SE image shown in Figure 4b. The highest stress should be located at the center of the cut (I), although this is clearly not represented by the signal intensity in Figure 4a. On the contrary, an increase of signal intensity is exhibited in regions where no increase of stress is expected on account of the sample shape (II in Figure 4a). The reason for this behavior is twofold. At first, the filter setting is chosen to suppress the signal originating from areas of high stress and to emphasize the signal originating from areas of moderate stress. The second reason is the weighting of the signal intensity with spin density and transverse relaxation. The thickness of the band decreases with increasing strain. Therefore, the spin density (i.e. the thickness of the rubber band, because the signal is integrated in the *z*-direction) and the signal intensity decrease with increasing stress. This behavior is amplified by the unavoidable T_2 weighting in the imaging sequence because T_2 decreases with increasing stress as well (cf. eq 4).[4,21]

The DQ weighted image can be corrected for the effects of spin density and transverse relaxation by dividing it by an SE image with the same T_2 dephasing time, yielding pure *double-quantum images*[27] for the individual filter setting. This is demonstrated in Figure 5a where images, similar to those of Figure 4, but with a filter setting which allows a qualitative interpretation, have been divided by each other. The contrast of Figure 5a is then determined only by the DQ coherence strength for the chosen DQ filter setting and is given by

$$S(\tau,\Delta\nu) \propto \sin(2\pi\tau\Delta\nu(\sigma)) \qquad (5)$$

In Figure 5b, a simulation by the finite element method (FEM) of the induced stress is shown in order to compare the information given in Figure 5a. The number of gray shades in Figure 5a has been reduced to five for reasons of better comparison. The region of highest stress is clearly located at the center of the cut, a behavior which is confirmed by the FEM simulation. The "butterfly" shaped distribution of stress in the areas surrounding the cut can clearly be identified in Figure 5a. Nevertheless, one has to keep in mind that the contrast in Figure 5a is still dependent on the DQ filter setting.

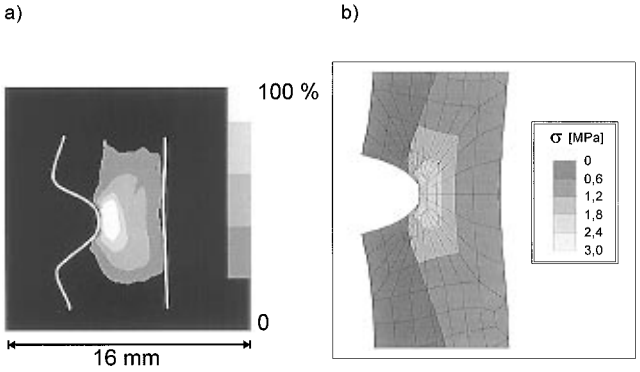

Figure 5. (a) DQ image of a strained band with one cut at $\lambda = 1.3$, corrected for spin density and relaxation effects. The DQ filter setting allows a qualitative evaluation of a stress map. The outline obtained from a spin-echo image is shown to indicate the sample shape. (b) FEM calculation of stress in a uniaxially stretched elastic band. The calculation was carried out with the material parameters of the elastic bands used in this work. Both methods show very similar stress distributions.

In order to obtain quantitative DQ parameter images, a whole set of DQ images has to be measured for different filter settings (preparation time τ of the DQ filter[27]). To extract $\Delta\nu$ for each pixel eq 4 has to be fitted to the data. A subsequent recalibration to stress by the master curve (cf. Figure 1b) should give the same result as determined by spectroscopic imaging (cf. Figure 2). The outcome of such an experiment is demonstrated in Figure 6, where a stretched rubber band with a cut on each side has been investigated at $\lambda = 1.5$. An example for a single DQ weighted image taken from the measured series is shown in Figure 6b, and the corresponding SE image with the same T_2 relaxation delay is shown in Figure 6a. A total of eight pairs of DQ weighted images and SE images was measured. Then, the DQ images were corrected by dividing each DQ weighted image by the corresponding SE image. Proceeding in this way, the pure DQ parameter image of Figure 6c was obtained from the images of Figure 6a,b. The resultant qualitative DQ image is sufficient to identify the area of high strain in the center of the band as well as the strain inhomogeneities close to the cuts. From the series of DQ images for different DQ filter settings, a fit of eq 5 to the data for each pixel yielded the *DQ parameter image* shown in Figure 6d. In this image the contrast is determined again by the quadrupole splitting. Finally, the contrast of this image was recalibrated to stress using the master curve in Figure 1b to obtain the stress parameter image shown in Figure 6e. Here, the highest stress is monitored in the middle of the sample with a value of about 4.7 MPa, whereas the stress decreases toward the sides. Although the absolute value of stress differs from that measured in the image of Figure 2b (bottom) due to the different width of the cuts in both samples, the strain distribution is consistent with the sample geometry and with the results of the spectroscopic imaging experiments shown in Figure 2.

Conclusion

The results of this work point out the benefits of using ^{2}H-NMR imaging for the analysis of stress in elastomers. The tedious synthesis of deuterated networks could be circumvented by the use of deuterated oligomers with a chemical structure compatible to that of the network chains. This reveals the possibility of using

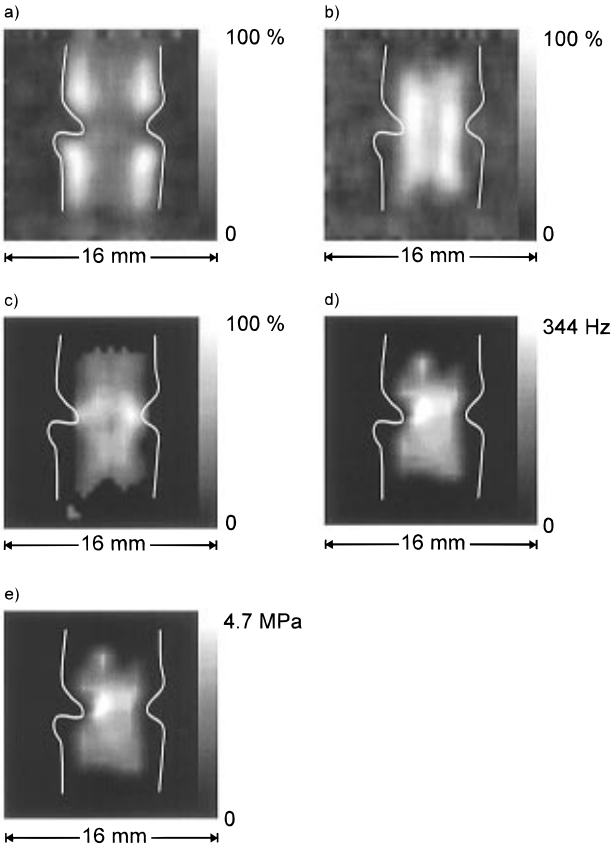

Figure 6. (a) Spin-echo image of a strained elastic band with a cut on each side at $\lambda = 1.5$. The contours in this and the following images correspond to the sample shape. (b) Double-quantum filtered image of the same sample. The DQ filter setting allows a qualitative evaluation of the image. The transverse relaxation delay is the same as in the spin-echo image shown in (a). (c) Result of dividing the DQ weighted image by the spin-echo image. By this procedure spin density as well as T_2 relaxation effects are eliminated. See text for details. (d) DQ parameter image, obtained by fitting eq 5 to the data of a set of eight differently weighted DQ images ($\tau =$ 200, 400, ..., 1400, 1600 μs). The contrast is determined by the quadrupole splitting. (e) Stress parameter image obtained by recalibration of the corresponding DQ parameter image with the master curve of Figure 1b.

the technique for studies on a larger scale. Elastomers, which are injection molded for example, seem to exhibit a high amount of chain order induced by the production process and represent an interesting field for new investigations.

Two methods for investigating stress distributions in uniaxially strained elastic bands were presented. Although both yield the same results, they have different sensitivities to local stress and different experimental advantages. A detailed description of the experimental differences and the differences in data processing is given elsewhere.[27]

The main disadvantage of spectroscopic 2D imaging is low sensitivity to small stress. In order to resolve the QS, its magnitude has to be greater than the line width of the isotropic signal at half-height. Therefore, only stress values of $\sigma \geq 1.2$ MPa can be measured by this method (see Figure 2b). However, advantages are easy experimental implementation, robustness, and straightforward data processing.

DQ imaging, on the other side, is a very sensitive method for the detection of small stress. However, problems arise when the data are fitted to eq 5 in order to calculate the QS from a series of corrected images. The fitting procedure becomes unstable for small stress, and the error in the calculated values for $\Delta\nu$ is large. A further disadvantage is the necessary acquisition of the second set of SE images and the tedious data processing.

The choice of the imaging technique to be used is a question not only of the sensitivity to various amounts of stress but also of measurement time. The acquisition of the stress parameter images required approximately 40 h, independent of the method used. If the information content of stress images does not need to be quantitative, the acquisition of DQ weighted images is sufficient for a qualitative interpretation and can be measured quite fast (typically 3 h). Of course special attention has to be given to the setting of the DQ filter. In order to rule out undesired effects of spin density variations and relaxation, these DQ weighted images need to be divided by SE images acquired with the same T_2 relaxation delay. Then, the sensitivity of DQ imaging for small anisotropies can be utilized although not quantitatively .

Finally, it is pointed out that the direction of local strain can be measured as well. The QS is a function of the angle Ψ between the direction of strain and the applied magnetic field (see eq 1), which was confirmed experimentally.[6,31] Therefore, if QS parameter images were measured in the *x,z*-plane, and the value of Ψ is incremented, an evaluation of the signal intensity of each pixel, according to P_2 (cos Ψ), should immediately give the direction of local strain.

Acknowledgment. The authors are grateful to Prof. Gil Navon, Tel Aviv, for pointing out the use of a double-quantum filter and for providing access to his work[32] prior to publication, and to Prof. Joel Miller, Washington, DC, for helpful discussions. We also thank Prof. Wolfram Gronski, Freiburg, Germany for providing the deuterated butadiene, and Prof. Michaeli, Aachen, Germany, for the stress−strain measurements and the FEM calculations. This research was supported by the Deutsche Forschungsgemeinschaft, grant no. BL 231/13-1.

References and Notes

(1) Blümich, B., Kuhn, W. Eds. *Magnetic Resonance Microscopy: Methods and Applications to Materials Science, Plants and Biomedicine*; VCH Publishers: Weinheim, 1992.
(2) Ackerman, J. L., Ellingson W. A., Eds. *Advanced Tomographic Imaging Methods for the Analysis of Materials*; Symposium Proceedings; Materials Research Society: 1990, Vol. 217.
(3) Blümler, P.; Blümich, B. *NMR Basic Princ. Prog.* **1994**, *30*, 209.
(4) Blümler, P.; Blümich, B. *Acta Polym.* **1993**, *44*, 125.
(5) Deloche, B.; Samulski, E. *Macromolecules* **1981**, *14*, 575.
(6) Deloche, B. *Proceedings of the European Workshop of Non-destructive Evaluation of Polymers* and *Polymer Matrix Composites*, Termar do Vimeiro Portugal; 1984.
(7) Chapellier, B.; Deloche, B.; Oeser, R. *J. Phys. II Fr.* **1993**, *3*, 1619.
(8) Deloche, B.; Samulski, E. T.; Beltzung, M. *J. Phys. Lett.* **1982**, *43*, 763.
(9) Deloche, B.; Dubault, A.; Herz, J.; Lapp, A. *Europhys. Lett.* **1986**, *1/12*, 629.
(10) Dubault, A.; Deloche, B.; Herz, J. *Polymer* **1984**, *25*, 1405.
(11) Dubault, A.; Deloche, B., Herz, J. *Macromolecules* **1987**, *20*, 2096.
(12) Stadler, R.; Jacobi, M. M.; Gronski, W. *Makromol. Chem., Rapid Commun.* **1983**, *4*, 129.
(13) Gronski, W.; Stadler, R.; Jacobi, M. M. *Macromolecules* **1984**, *17*, 741.
(14) Jacobi, M. M.; Stadler, R.; Gronski, W. *Macromolecules* **1986**, *19*, 2884.
(15) Jacobi, M. M. Ph.D. Thesis, Freiburg, Germany, 1989 (in German).

(16) Gronski, W.; Hoffmann, U.; Simon, G.; Wutzler, A.; Straube, E. *Rubber Chem. Technol.* **1991**, *65*, 63.
(17) Jacobi, M. M.; Abetz, V.; Stadler, R.; de Lucca Freitas, L.; Gronski, W. *Colloid Polym. Sci.* **1995**, *273*, 544.
(18) Simon, G. *Polym. Bull.* **1991**, *25*, 365.
(19) Simon, G.; Birnstiel, A.; Schimmel, K.-H. *Polym. Bull.* **1989**, *21*, 235.
(20) Simon, G.; Götschmann, B.; Matzen, D.; Schneider, H. *Polym. Bull.* **1989**, *21*, 475.
(21) Simon, G.; Baumann, K.; Gronski, W. *Macromolecules* **1992**, *25*, 3624.
(22) Simon, G.; Schneider, H. *Makromol. Chem., Macromol. Symp.* **1991**, *52*, 233.
(23) Sotta, P.; Deloche, B.; Herz, J.; Lapp, A.; Durand, D.; Rabadeux, J.-C. *Macromolecules* **1987**, *20*, 2769.
(24) Günther, E.; Blümich, B.; Spiess, H. W. *Mol. Phys.* **1990**, *71*, 477.
(25) Günther, E.; Blümich, B.; Spiess, H. W. *Chem. Phys. Lett.* **1991**, *184*, 251.
(26) Cockman, M.; Jelinski, L.; Katz, J.; Sorce, D.; Boxt, L.; Cannon, P. *J. Magn. Reson.* **1990**, *90*, 9.
(27) Klinkenberg, M.; Blümler, P.; Blümich, B. *J. Magn. Reson. A* **1996**, *119*, 197.
(28) Kimmer, W.; Schmalz, E. O. *Kautsch. Gummi Kunstst.* **1963**, *16*, 606.
(29) Ogden, R. W. *Proc. R. London* **1972**, *A326*, 565.
(30) Bax, A.; Freeman, R.; Kempsell, S. B. *J. Am. Chem. Soc.* **1980**, *102*, 4849.
(31) Klinkenberg, M. Ph.D. Thesis, Aachen, Germany **1996**, (in German).
(32) Sharf, Y.; Eliav, U.; Shinar, H.; Navon, G. *J. Magn. Reson., Ser. B* **1995**, *107*, 60.

MA9608176